JOC The Journal of Organic Chemistry

Article

pubs.acs.org/joc

Theoretical Studies on the Regioselectivity of Iridium-Catalyzed 1,3-Dipolar Azide–Alkyne Cycloaddition Reactions

Qiong Luo,[†,‡] Guochen Jia,*[,†] Jianwei Sun,*[,†] and Zhenyang Lin*[,†]

[†]Department of Chemistry, The Hong Kong University of Science and Technology, Clear Water Bay, Kowloon, Hong Kong, P. R. China

[‡]MOE Key Laboratory of Theoretical Environmental Chemistry, Center for Computational Quantum Chemistry, South China Normal University, Guangzhou 510631, P. R. China

Supporting Information

ABSTRACT: Iridium-catalyzed cycloaddition of thioalkynes and bromoalkynes with azides have been investigated with the aid of density functional theory (DFT) calculations at the M06 level of theory. Our investigation focused on the different regioselectivity observed for the reactions of the two classes of alkynes. The DFT results have shown that the mechanisms of cycloaddition reactions using thioalkynes and bromoalkynes as substrates are similar yet different. The reactions of thioalkynes occur via a metallabicyclic Ir–carbene intermediate formed through alkyne–azide oxidative coupling via attack of the azide terminal nitrogen toward the β alkyne carbon, whose carbene ligand is stabilized by an alkylthio/arylthio substituent. Reductive elimination from the intermediate leads to the formation of the experimentally observed 5-sulfenyltriazole. In the reactions of bromoalkynes RC≡CBr, the reaction mechanism involves the initial formation of a six-membered-ring metallacycle intermediate in the oxidative coupling step. The six-membered-ring intermediate then undergoes isomerization via migrating the terminal azide nitrogen from the β carbon to the α carbon to form a much less stable metallabicyclic Ir–carbene species from which reductive elimination gives 4-bromotriazole.

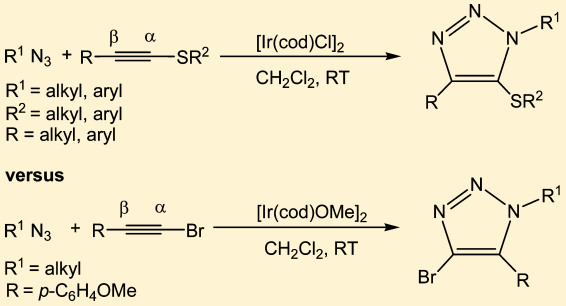

INTRODUCTION

1,2,3-Triazoles represent a significant class of nitrogen heterocyclic compounds that have been widely used in various applications ranging from pharmaceuticals[1] to materials.[2] 1,3-Dipolar azide–alkyne cycloadditions (AACs) catalyzed by various transition-metal complexes provide an atom-economical method for the regiocontrolled synthesis of differently substituted 1,2,3-triazoles.[3−5] Among them, copper-catalyzed AACs (CuAACs) are the most efficient one to selectively construct 1,4-disubstituted 1,2,3-triazole rings.[3,6] It has been suggested that the reaction mechanism of CuAACs involves a copper acetylide as the active species in the catalytic cycle in the presence of a base.[6,7] Altough CuAACs have received tremendous attention, they are largely limited to terminal alkynes (including metal acetylides) and activated haloalkynes.[3,8]

Ruthenium-catalyzed AACs (RuAACs) were found to be applicable to both terminal and internal alkynes for the synthesis of fully substituted 1,2,3-triazoles.[4] Complementary to the CuAACs, the RuAACs of terminal alkynes regioselectively give 1,5-disubstituted 1,2,3-triazoles.[4] The proposed mechanism, which accounts for the RuAACs, involves oxidative coupling of azide and alkyne to give a ruthenacycle, followed by reductive elimination. DFT calculations supported the proposed mechanism and indicated that the regioselectivity is determined by the oxidative coupling step, which can be viewed as a nucleophilic attack of the activated alkyne on the electrophilic terminal nitrogen of the coordinated azide.[4c]

Very recently, it has been reported that $[Ir(cod)Cl]_2$ can catalyze cycloaddition of azides with internal thioalkynes to give 5-sulfenyltriazoles with excellent regioselectivity (eq 1)[9] by

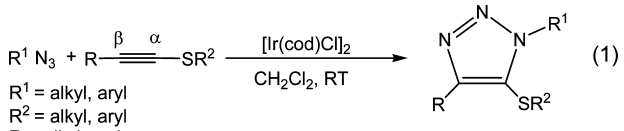

(1)

(2)

using dichloromethane as the solvent at room temperature. The regioselectivity was suggested to be a result of thio-coordination to the iridium center during the catalytic reaction (Scheme 1).

Special Issue: Mechanisms in Metal-Based Organic Chemistry

Received: August 8, 2014
Published: September 15, 2014

Scheme 1

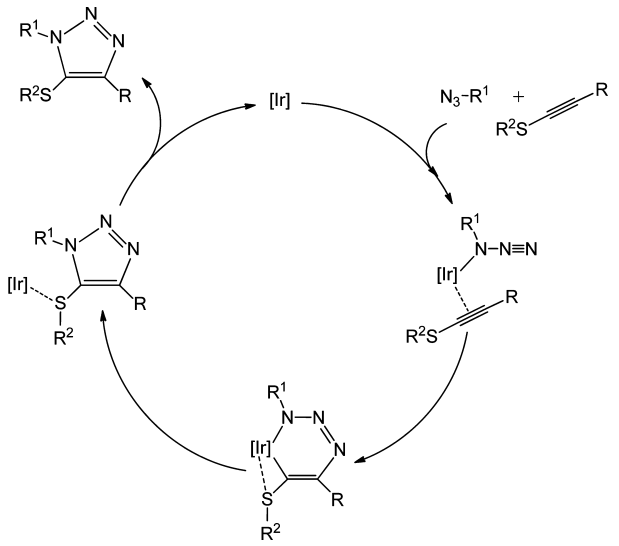

In another report, related Ir-catalyzed AACs of 1-bromoalkynes using $[Ir(cod)OMe]_2$ as the catalyst give completely different regioselectivity under similar experimental conditions[10] when compared with those of thio-alkynes (eq 1 versus eq 2). The reason for the different regioselectivity is not clear. Therefore, it is necessary to carry out a systematic theoretical study on the mechanisms of the IrAACs in order to have a full picture of the reaction mechanisms and to understand the factor influencing the observed regioselectivities.

COMPUTATIONAL DETAILS

All the molecular geometries and energies presented in this study were computed using the M06 level of density functional theory.[11] The effective core potentials (ECPs) of Hay and Wadt with double-ζ valence basis sets (LanL2DZ)[12] were employed to describe Ir. The 6-31G(d) basis set was used for N, S, Cl, Br, and O as well as the C atoms in the triple bonds of alkynes and double bonds of 1,5-cyclooctadiene (cod). The 6-31G basis set was used for all other atoms. Frequency calculations were performed at the same level to identify all stationary points as minima or transition states and to provide relative free energies at 298.15 K. Intrinsic reaction coordinates (IRC)[13] were carried out to identify transition states connecting two relevant minima. Natural bond orbital (NBO) analysis[14] was performed for the structures of $\mathbf{Br\_C3}_{PMP}$ and $\mathbf{Br\_C31'}_{PMP}$ at the same level of theory to understand the origin of the significant stability of $\mathbf{Br\_C3}_{PMP}$ compared to $\mathbf{Br\_C31'}_{PMP}$.

To examine whether the above employed basis set is sufficient, we performed single-point calculations on the transition-state structures involved in the oxidative coupling step shown in Figure 2 using the 6-311+G(d,p) basis set for the main group atoms and LanL2DZ basis set with added polarization function $\zeta(f) = 0.938$ for Ir. In addition, the solvation effect on the calculation results was also examined by performing solvation energy calculations using the SMD (solvation model density) solvent model with dichloromethane as the solvent.[15] These additional calculations show that the level of theory we used is reliable for the systems studied in this work. For example, with the higher level (better basis set plus solvation energy included) of calculations, the free energy barriers calculated for the oxidative coupling steps **B1** → **C1**, **B2**→ **C2**, **B3** → **C3**, **B4** → **C4**, and **B4** → **C4′** are 32.8, 35.4, 14.4, 16.1, and 17.8 kcal/mol, respectively. These barriers do not differ significantly from those presented in Figure 2.

All the calculations were performed with the Gaussian 09 software package.[16]

RESULTS AND DISCUSSION

Ir-Catalyzed Cycloaddition of Thioalkynes with Azides. *Active Species.* The experimental results indicated that the Ir-catalyzed cycloaddition reactions of thioalkynes with azides are not sensitive to substituents on the substrates (eq 1).[9] Thus, we first considered the simple model substrates MeC≡CSMe and N_3-Me, which have all methyl groups as the substituents. We hypothesize that the IrAACs start with a facile fragmentation of the precatalyst $[Ir(cod)Cl]_2$ in the presence of the substrates, alkynes and azides, to give the active species $[Ir(cod)Cl(MeC{\equiv}CSMe)]$ or $[Ir(cod)Cl(N_3Me)]$. We choose $[Ir(cod)Cl(MeC{\equiv}CSMe)]$ (**A**) as the active species based on our calculation results that MeC≡CSMe binds with Ir(cod)Cl more strongly than N_3Me does by 4.0 kcal/mol.

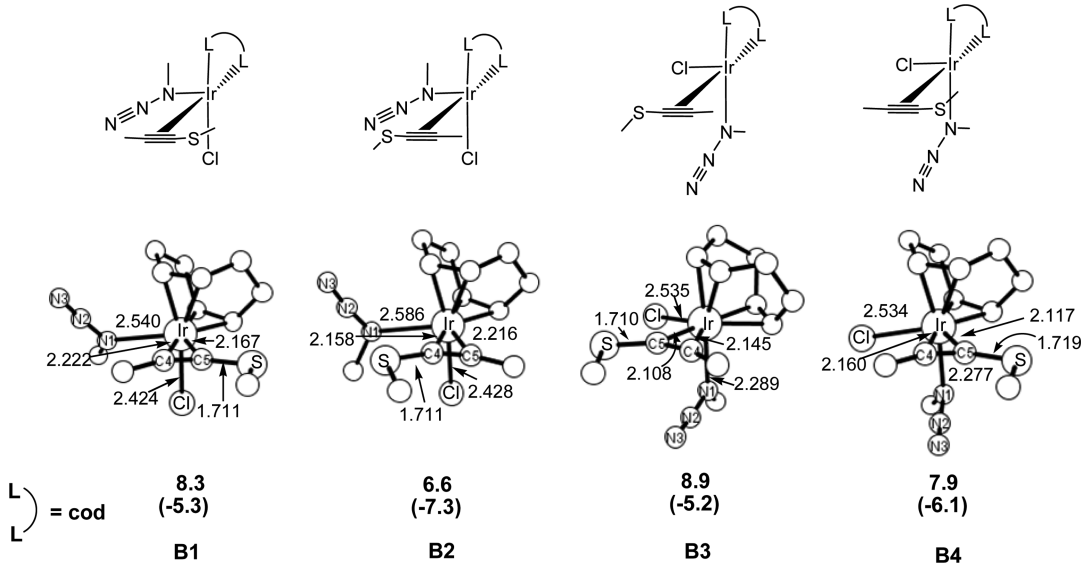

Figure 1. Optimized structures for the four structural isomers of the active species $[Ir(cod)Cl(MeC{\equiv}CSMe)(N_3Me)]$ (**B**) with selected structural parameters (bond lengths in angstroms). The computed relative free energies and electronic energies (in parentheses) are given in kcal/mol taking the square planar complex $[Ir(cod)Cl(MeC{\equiv}CSMe)]$ (**A**) + methyl azide as the reference energy point. Hydrogen atoms are omitted for clarity.

dx.doi.org/10.1021/jo5018348 | J. Org. Chem. 2014, 79, 11970−11980

Starting from the active species [Ir(cod)Cl(MeC≡CSMe)] (**A**), complexation of the model substrate molecule N_3Me gives the 18-electron species [Ir(cod)Cl(MeC≡CSMe)(N_3Me)] (**B**). Four possible structural isomers of **B** were obtained on the basis of our calculations, as shown in Figure 1.

It is well-known that, for an 18-electron ML_5 complex, both trigonal-bipyramidal (TBP) and square-pyramidal (SQP) structures are possible.[17] In our calculations, various initial TBP structures of **B** were used for geometry optimizations. All the optimizations eventually give SQP structures. This result is likely due to the rigidity of the cod ligand. The apical position in each of the SQP structures, in principle, can be occupied by any type of ligands. Previous investigations indicated that weak trans-influencing ligands preferentially occupy the apical position in an 18-electron SQP ML_5 complex.[18] This is because the trans position of the apical ligand is no longer exactly "vacant" but instead is occupied by a pair of metal d electrons. This pair of metal d electrons is the strongest *trans*-influence "ligand" as discussed in literature.[18] Indeed, the structural isomers obtained for [Ir(cod)Cl(MeC≡CSMe)(N_3Me)] (**B**) (Figure 1) have either N_3Me or Cl^- at the apical position. Methyl azide can coordinate to the metal center via the nitrogen proximal to carbon or via the terminal nitrogen atom. Although both modes of coordination are known, the former is by far more commonly observed.[19,4a] Alkyne can also coordinate to the metal center in a π-fashion in two distinct orientations. All the analyses above explain why the four structural isomers (**B1**, **B2**, **B3**, and **B4** in Figure 1) were obtained in our calculations for [Ir(cod)Cl(MeC≡CSMe)(N_3Me)] (**B**).

Oxidative Coupling. On the basis of the mechanism shown in Scheme 1, oxidative coupling of azide with alkyne to give an iridacycle is the first step for the reaction to proceed. The oxidative coupling where a new carbon−nitrogen bond is formed between the terminal nitrogen of azide and the β (aryl-/alkyl substituted) carbon of alkyne would eventually lead to the experimentally observed product 5-sulfenyltriazole. Otherwise, 4-sulfenyltriazole would be obtained. In terms of molecular geometries of the four structural isomers (Figure 1), the β alkyne carbon in **B1** is available for the attack of the terminal nitrogen of the azide to form new carbon−nitrogen bond, while in **B2** the α (methylthio-substituted) alkyne carbon is accessible for such attack. In **B3** and **B4**, both alkyne carbons can take part in the oxidative coupling process. Therefore, starting from the four structural isomers, there are six possible pathways for the oxidative coupling to eventually give 5/4-sulfenyltriazole.

We calculated the energy profiles for the possible oxidative couplings as shown in Figure 2. The free energy barriers for ligand dissociation/association processes (e.g., **A** to **B1** and **A** to **B2** in Figure 2a,b) were calculated according to the method proposed by Hall and co-workers.[20,21] The oxidative couplings in **B1** and **B2** lead to the formation of the six-membered ring metallacycle **C1** and **C2**, with overall free energy barriers of 28.4 and 30.3 kcal/mol, respectively.

From **B3**, the free energy barrier (with respect to the energy reference point) for the oxidative coupling between the terminal nitrogen of azide and the β alkyne carbon to give the metallabicyclic Ir−carbene intermediate **C3** was calculated to be 12.0 kcal/mol (Figure 2c). Unexpectedly, we were not able to locate a transition state for the oxidative coupling between the terminal nitrogen of azide and the α alkyne carbon, which links **B3** and the metallabicyclic Ir−carbene intermediate **C3′** (Figure 4). We were also unable to locate the corresponding six-membered ring metallacycle structural isomer of **C3**, where the terminal nitrogen of the azide bonded to the β alkyne carbon.

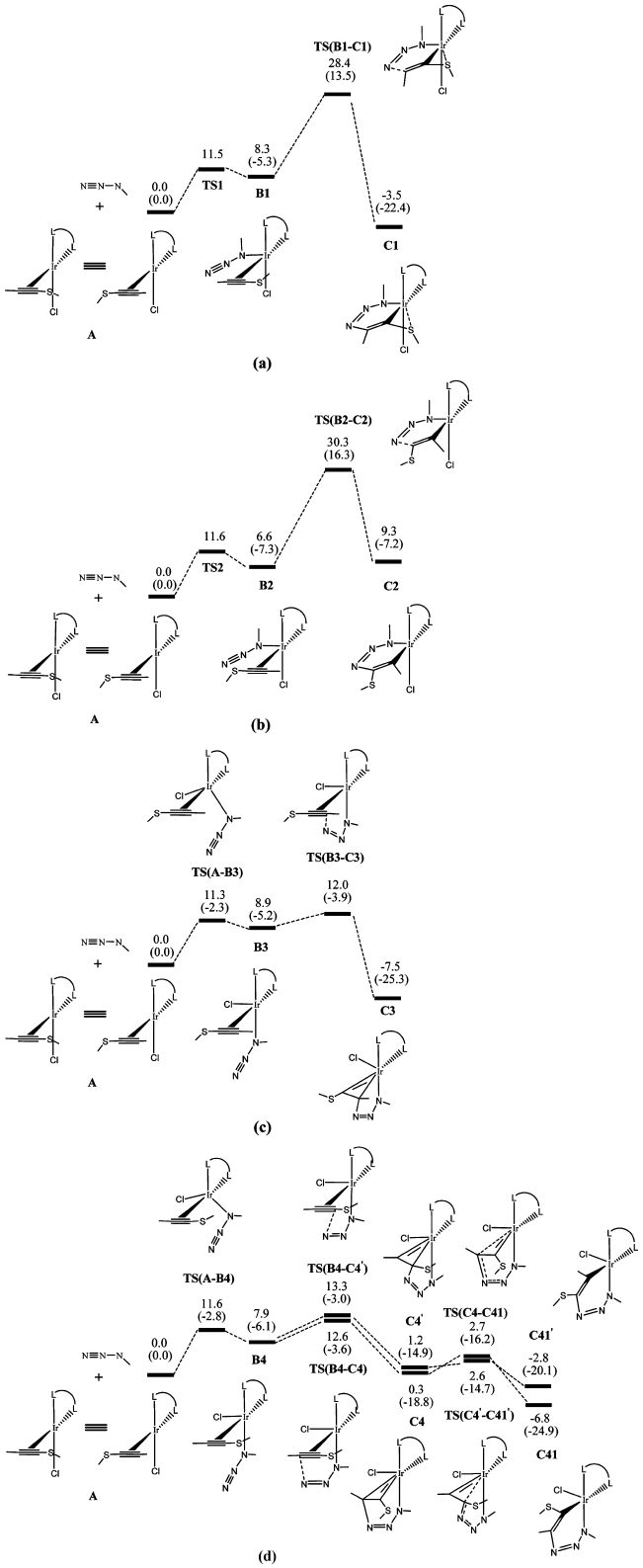

Figure 2. Energy profiles calculated for the oxidative coupling via **B1** (a), **B2** (b), **B3** (c), and **B4** (d). The relative free energies and electronic energies (in parentheses) are given in kcal/mol.

dx.doi.org/10.1021/jo5018348 | J. Org. Chem. 2014, 79, 11970−11980

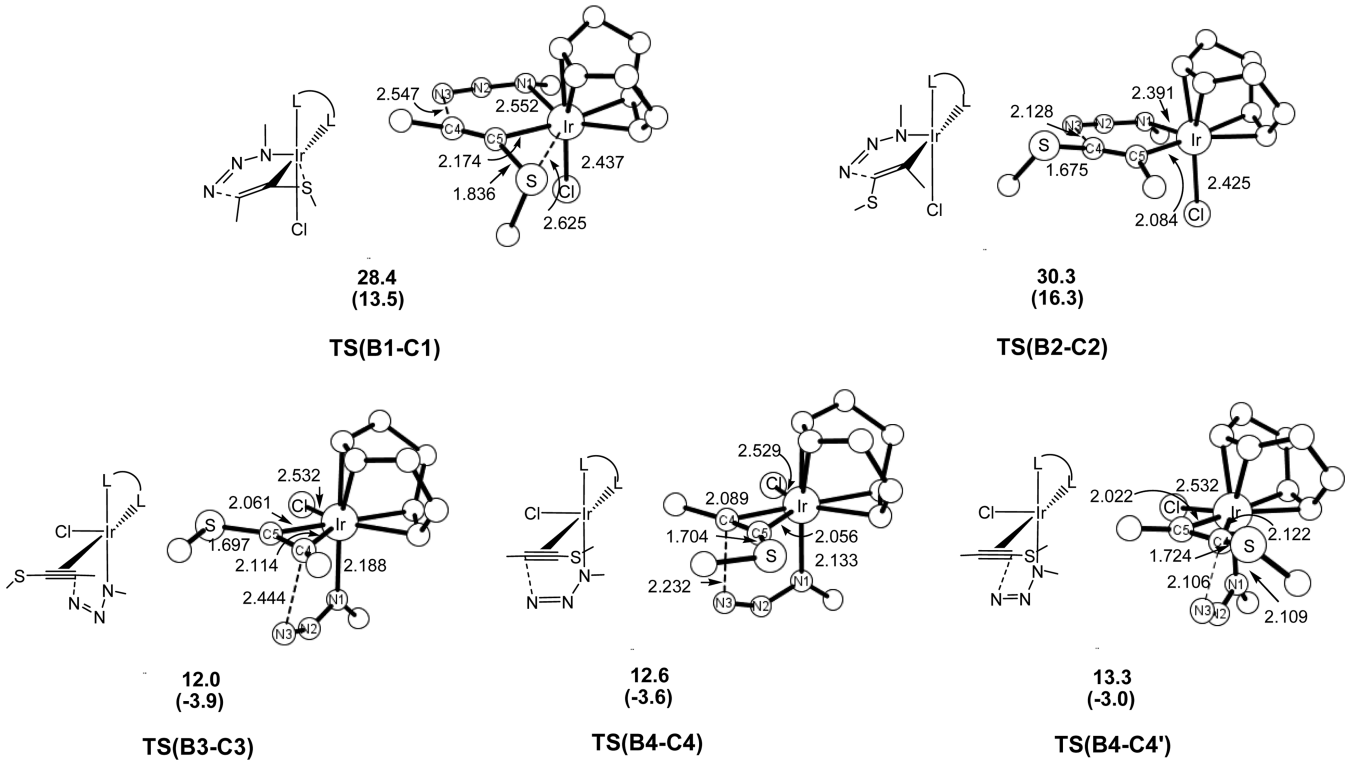

Figure 3. Optimized structures of the transition states for the oxidative couplings shown in Figure 2 with selected structural parameters (bond lengths in angstroms). The relative free energies and electronic energies (in parentheses) are given in kcal/mol. Hydrogen atoms are omitted for clarity.

From **B4**, interestingly, both the transition states for the oxidative couplings between the terminal nitrogen of azide and both the α and β alkyne carbons can be located. The oxidative couplings occurring via the attack of the terminal nitrogen of azide to the β and α alkyne carbons to give the metallabicyclic Ir−carbene intermediate **C4** and **C4′**, respectively, are competitive with overall free energy barriers of 12.6 and 13.3 kcal/mol, respectively. Different from **C3**, the metallabicyclic Ir−carbene intermediate **C4** and **C4′** can further isomerize to the more stable corresponding six-membered ring metallacycles **C41** and **C41′**, respectively (Figure 2d).

The calculated results shown in Figure 2 indicate that the oxidative couplings via **B1** and **B2** show significantly higher barriers than those via **B3** and **B4** (Figure 2). The significantly high free energy barriers for the oxidative couplings are of the following electronic origin. It is noticed that the Ir−N(azide) bonds in **B1** and **B2** (as well as **TS(B1−C1)** and **TS(B2−C2)**) are significantly longer than those in **B3** and **B4** (as well as **TS(B3−C3)** and **TS(B4−C4)**/ **TS(B4−C4′)**) (Figures 1 and 3), a result of the very strong trans influencing "ligand" (a pair of metal d electrons) occupying the position trans to the apical azide ligand as mentioned above.[18] Because of the much weaker interaction between azide and the metal center in **B1** and **B2**, we conveniently expect that the azide ligands in **B1** and **B2** are much less activated by the metal center, and therefore, the related couplings are more energetically demanding. An alternative explanation for the low barriers for the oxidative couplings via **B3** and **B4** can be as follows. The relative orientation of alkyne and azide does not change significantly during the conversion from **B3** or **B4** to **C3** or **C4**/**C4′**, facilitating the transfer of the metal electrons occupying the d_{z2} orbital to the alkyne/azide moiety and thus giving rise to low barriers. Here, the z axis is defined along the Ir−Cl bond.

Before we continue our discussion we would like to comment briefly on the relative stability of **C1** and **C2**. Figure 4 shows the calculated structures. **C1** and **C2** are similar in their structures. However, **C1** is significantly more stable than **C2**. The higher stability of **C1** can be attributed to the additional interaction between the methylthio and the metal center, evidenced by the short Ir---S contact (2.661 Å) and small Ir−C(5)−S angle (89.9°).

The next issue that needs to be addressed here is the origin of the relative preference for oxidative couplings from **B3** and **B4**. In an early study of Ru-catalyzed cycloaddition,[4c] it was noted that oxidative coupling between an internal-nitrogen-coordinated azide and a coordinate alkyne can be considered as an electrophilic attack of the terminal nitrogen of the azide to one of the two coordinated alkyne carbons. In the current study, the methyl-substituted β carbon of the coordinated alkyne is expected to be more π electron-rich than the methylthio-substituted α carbon because of the strong π-donating property of a methylthio substituent, which might explain why the transition state for the oxidative coupling via **B3** between the terminal nitrogen of azide and the α alkyne carbon cannot be located. However, the same argument seems not to work when we come to understand the two oxidative coupling pathways calculated for **B4**. The structure of **B4** is very similar to that of **B3** except in the relative orientation of the coordinated alkyne. With the same argument, it is expected that the α alkyne carbon should be much less reactive toward oxidative coupling and that we might not be able to locate the transition state for the oxidative coupling between the terminal nitrogen of azide and the α alkyne carbon as what we have seen

dx.doi.org/10.1021/jo5018348 | J. Org. Chem. 2014, 79, 11970−11980

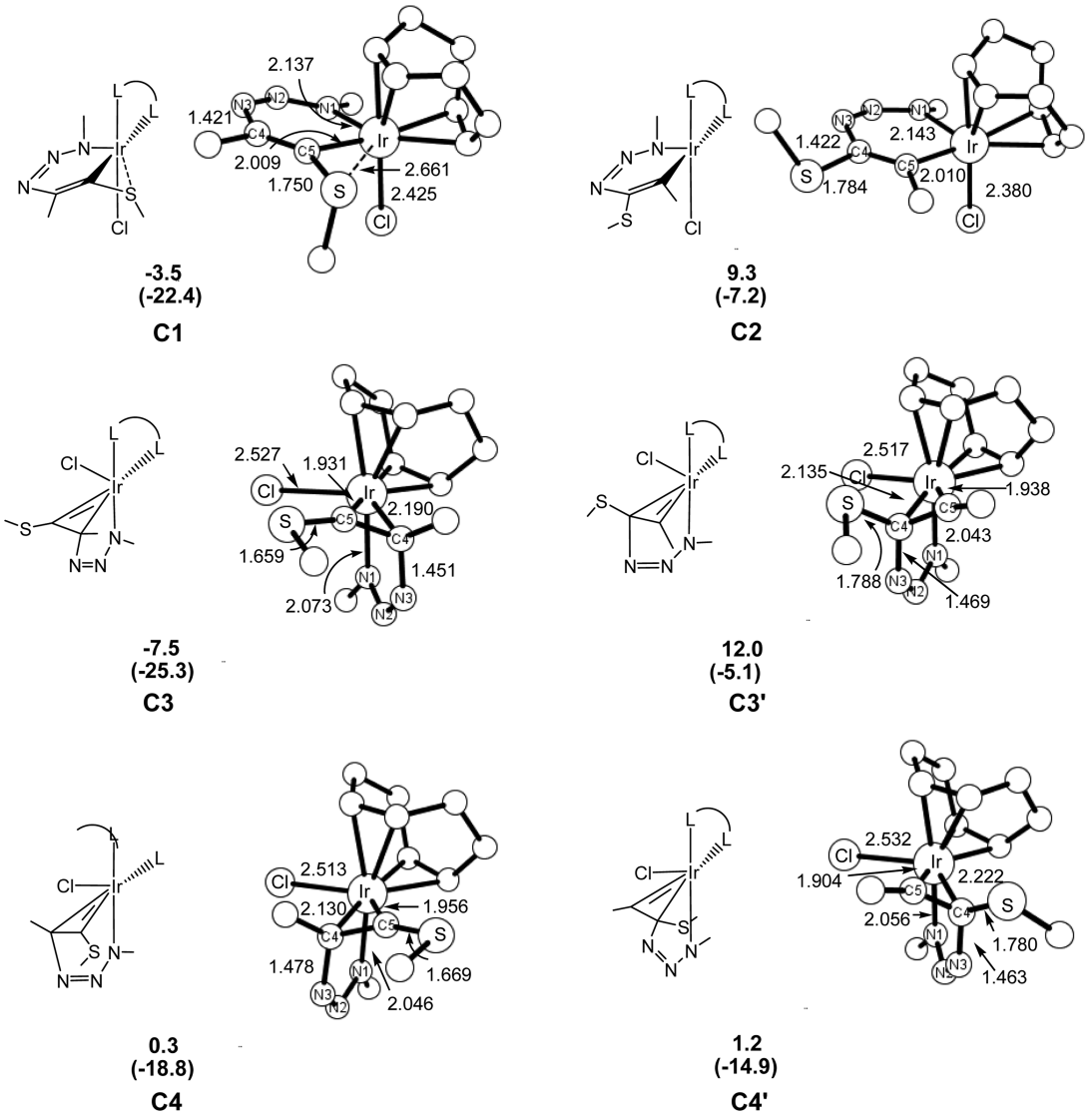

Figure 4. Optimized structures of the intermediates derived from the oxidative couplings with selected structural parameters (bond lengths in angstroms). The relative free energies and electronic energies (in parentheses) are given in kcal/mol. Hydrogen atoms are omit for clarity.

for **B3**. However, from Figure 2d, we were surprised to see that both the α and β alkyne carbons are comparably reactive toward oxidative coupling. These results imply that the relative π-electron richness of the α and β alkyne carbons does not have a crucial influence on the preference of the attack of the azide terminal nitrogen toward the β or α carbon in **B3** and **B4**.

Although the transition state for the oxidative coupling via **B3** between the terminal nitrogen of azide and the α alkyne carbon cannot be located, we were able to locate the relevant metallabicyclic Ir−carbene intermediate **C3′** (Figure 4), which has the terminal nitrogen of azide bonded to the α alkyne carbon, as a minimum on the potential energy surface. Inspite of their similarity in structure, **C3′** is significantly less stable than **C3** by 19.5 kcal/mol (Figure 4). The highly unstable **C3′** should be related to the failure of locating a transition state linking **B3** and **C3′**. There are two factors affecting the stability of **C3′**. One factor is that the ligand arrangement in **C3′** does not allow an optimal metal−carbene interaction; i.e., the metal−carbene bond is not perfectly lying along one of the octahedral axes. The other factor is that the carbene ligand in **C3′** is not stabilized by the π-donating methylthio substituent. **C3** shows significant stability because its structure allows optimal metal−carbene interaction with the metal−carbene bond lying along one of the octahedral axes and the carbene ligand is stabilized by the π-donating methylthio substituent.

The free energy barriers calculated for the two oxidative couplings via **B4** are very close to each other and slightly higher than that calculated for the oxidative coupling from **B3** (Figure 2c, d). The metallabicyclic Ir−carbene intermediates **C4** and **C4′** are also very close to each other in energy and are less stable than **C3** by ca. 8 kcal/mol. In **C4**, the structure does not allow an optimal metal−carbene interaction, but the carbene ligand is stabilized by the π-donating methylthio substituent (Figure 4). In **C4′**, the structure allows an optimal metal−carbene interaction but the carbene ligand is not stabilized by the π-donating methylthio substituent (Figure 4).

Reductive Elimination. Figure 2c,d shows that the diffirences are not notable among the free energy barriers for the three oxidative couplings from **B3** and **B4**. Therefore, it is necessary to perform calculations systematically for various reductive elimination pthaways leading to the cycloaddition of MeC≡CSMe with N_3-Me from **C3**, **C4** ,and **C4′**.

dx.doi.org/10.1021/jo5018348 | J. Org. Chem. 2014, 79, 11970−11980

Figure 5a shows the energy profile calculated for the reductive elimination step from **C3**. We can see that the

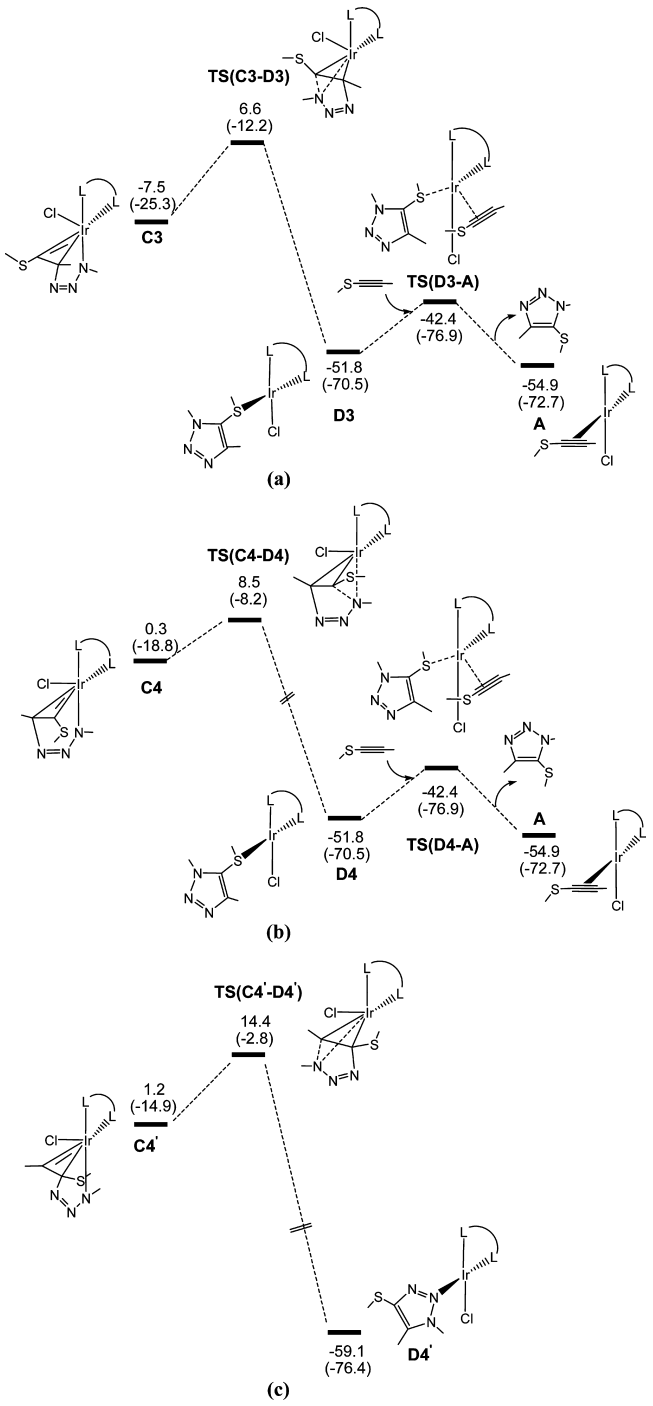

Figure 5. Energy profiles calculated for the reductive elimination via **C3**, **C4**, and **C4′**. The relative free energies and electronic energies (in parentheses) are given in kcal/mol. **D3** and **D4** are the same species. They are labeled differently for the convenience of discussion.

metallabicyclic Ir−carbene intermediate **C3** undergoes reductive elimination to give the metal−triazole complex **D3** with a free energy barrier of 14.1 kcal/mol. Starting from **D3**, a ligand substitution of alkyne-for-triazole with a barrier of 9.4 kcal/mol releases the cycloaddition product molecule (5-sulfenyltriazole) and regenerates the active species **A**. The overall catalyzed cycloaddition reaction to give 5-sulfenyltriazole is exergonic by −54.9 kcal/mol. The reductive elimination is the rate-determining step with an overall reaction barrier of 14.1 kcal/mol. As mentioned above, other than **C3**, the corresponding six-membered ring metallacycle structural isomer where the terminal nitrogen of the azide bonded to the β alkyne carbon does not correspond to a local minimum on the potential energy surface.

In Figure 5b, **C4** undergoes a facile reductive elimination to give the metal−triazole complex **D4** (here **D4** is the same as **D3** in Figure 5a; we use a different label for the purpose of clarity in the discussion) with a free energy barrier of 8.2 kcal/mol. Subsequent ligand exchange of alkyne-for-triazole gives 5-sulfenyltriazole and regenerates the active species **A** with a free energy barrier of 9.4 kcal/mol. Combining Figures 2d and 5b, we can see that the overall barrier for the pathway via **B4** then **C4** to gives 5-sulfenyltriazole is 15.3 kcal/mol, which corresponds to the energy difference between **TS(C4−D4)** and **C41**.

Figure 5c shows that the energy profile calculated for the reductive elimination from **C4′** via **TS(C4′-D4′)** to give a 4-sulfenyltriazole regioisomer is much less favorable with the relative free energy of **TS(C4′-D4′)** higher than **TS(C3-D3)** and **TS(C4-D4)** by 7.8 and 5.9 kcal/mol, respecively.

Summarizing the results presented in Figures 2 and 5, we conclude that the pathways **A** + N_3Me → **B3** → **C3** → **D3** → **A** + 5-sulfenyltriazole and **A** + N_3Me → **B4** → **C4** (**C41**) → **D4** → **A** + 5-sulfenyltriazole (slightly less favorable) are responsible for the regioselective outcome observed experimentally in the catalytic reactions shown in eq 1.[9] In other words, the reaction mechanism for the IrAACs (eq 1) consists of the following four steps (Figures 2 and 5): (i) complexation of azide to the active species **A** leading to **B3** or **B4** in which both the azide and alkyne substrate molecules are coordinated to the Ir(I) metal center; (ii) subsequent oxidative coupling between the terminal nitrogen of azide and the methyl-substituted carbon of MeC≡CSMe to give the metallabicyclic Ir−carbene intermediate **C3** or **C4** (**C41**); (iii) reductive elimination to give the intermediate **D3** or **D4** where the cycloaddition product molecule is a ligand; and (iv) finally ligand substitution of alkyne for the triazole product molecule to regenerate the active species **A**.

The experimental results indicated that the catalytic reactions shown in eq 1 are applicable to a wide scope of the thioalkyne substrates.[9] Thus, we also calculated the potential energy profiles based on the above-mentioned mechanism by using RC≡CSMe (R = Ph and *p*-C_6H_4OMe) as the substrates.

The energy profiles calculated for the Ir-catalyzed cycloaddition of RC≡CSMe (R = Ph and *p*-C_6H_4OMe) with N_3-Me are presented in the Supporting Information (Figures S1 and S2). Interestingly, for RC≡CSMe (R = Ph and *p*-C_6H_4OMe), the pathways to the formation of $\mathbf{B4}_{Ph}$ and $\mathbf{B4}_{PMP}$ are more favorable than those of $\mathbf{B3}_{Ph}$ and $\mathbf{B3}_{PMP}$ due to the steric effects caused by the Ph and *p*-C_6H_4OMe groups. The favorable energy profiles were found to proceed via $\mathbf{B4}_{Ph}$ and $\mathbf{B4}_{PMP}$ (Figures S1(b) and S2(b), Supporting Information). For both thioalkyne substrates RC≡CSMe (R = Ph and *p*-C_6H_4OMe), the calculated results show that the pathways to give 5-sulfenyltriazole are much more favorable than those to produce the 4-sulfenyltriazole regioisomer.

It is interesting to note that the reactions of MeC≡CSMe, PhC≡CSMe, and RC≡CSMe (R = *p*-C_6H_4OMe) give the same regioselectivity despite the different electronic properties among Me, Ph, and *p*-C_6H_4OMe. These results are due to the

dx.doi.org/10.1021/jo5018348 | J. Org. Chem. 2014, 79, 11970−11980

fact that the methylthio substituent is far stronger in its π-donating ability when compared with Me, Ph, and p-C_6H_4OMe.

The above computational results are in good agreement with the experimental observations.[9] Based on these results, our proposed mechanism describes the regioselectivity of the Ir-catalyzed cycloaddition reactions of azides with internal thioalkynes shown in eq 1. An alkylthio/arylthio substituent is able to stabilize the metallabicyclic Ir−carbene intermediate formed from the Ir-mediated azide−alkyne oxidative coupling through attack of the azide terminal nitrogen toward the β alkyne carbon and facilitate the immediately following reductive elimination to give the experimentally observed regioselective isomer 5-sulfenyltriazole.

Ir-Catalyzed Cycloaddition of Bromoalkynes with Azides. *Oxidative Coupling.* Equation 2 shows that the Ir-catalyzed cycloaddition reactions of bromoarylalkynes with azides give 4-bromotriazoles, whose regioselectivity is different from the cycloaddition reactions of thioalkynes.[10] Experimentally, it was shown that cycloaddition reactions of electron-rich bromoarylalkyne PMPC≡CBr (PMP = p-C_6H_4OMe) were most efficient.[10] Here, we report our calculated energy profiles for the model reaction of PMPC≡CBr with N_3Me employing $[Ir(cod)OMe]_2$ as the catalyst.

Coordination of both N_3Me and PMPC≡CBr to the metal center gives the 18-electron species **Br_B$_{PMP}$**. Similarly, four structural isomers (**Br_B1$_{PMP}$**, **Br_B2$_{PMP}$**, **Br_B3$_{PMP}$**, and **Br_B4$_{PMP}$**) were found for the 18-electron species **Br_B$_{PMP}$**. We first considered the oxidative coupling pathways from the four structural isomers.

Figure 6 shows calculated energy profiles for the oxidative couplings via the four structural isomers **Br_B1$_{PMP}$**, **Br_B2$_{PMP}$**, **Br_B3$_{PMP}$**, and **Br_B4$_{PMP}$**. Similar to what we have seen in the reaction of thioalkyne, when N_3Me occupies the apical position (**Br_B1$_{PMP}$** and **Br_B2$_{PMP}$**), the oxidative coupling shows a significantly high barrier. Again, N_3Me is less activated when it occupies the apical position in the 18-electron square-pyramidal complex, giving rise to a high barrier in the oxidative coupling.

For the oxidative coupling pathways via **Br_B3$_{PMP}$** and **Br_B4$_{PMP}$** (Figure 6c, d), the results are different from what we have seen for those in the reaction of thioalkyne. There are two oxidative coupling pathways calculated for **Br_B3$_{PMP}$** (Figure 6c), instead of one as seen for **B3** (Figure 2c), and there is only one oxidative coupling pathway calculated for **Br_B4$_{PMP}$** (Figure 6d), instead of two as seen for **B4** (Figure 2d). From Figure 6c,d, it can also be seen that attack of the terminal nitrogen of the coordinated-azide to the β (aryl-substituted) alkyne carbon in **Br_B3$_{PMP}$** to give a six-membered-ring metallacycle intermediate **Br_C3$_{PMP}$** is the most favorable with a free energy barrier of 13.5 kcal/mol. All these results can again be conveniently related to the relative stability of the intermediates (**Br_C1$_{PMP}$**, **Br_C2$_{PMP}$**, **Br_C3$_{PMP}$**, **Br_C3′$_{PMP}$**, and **Br_C4′$_{PMP}$**) derived from the oxidative couplings. The most favorable oxidative coupling pathway corresponds to that giving the most stable intermediate **Br_C3$_{PMP}$**.

In the five intermediates, two have metallabicyclic Ir−carbene structures (**Br_C3′$_{PMP}$** and **Br_C4′$_{PMP}$**) and three contain six-membered ring structures (**Br_C1$_{PMP}$**, **Br_C2$_{PMP}$**, and **Br_C3$_{PMP}$**). Interestingly, we do not see a metallabicyclic Ir−carbene structure in which the carbene ligand is stabilized by a bromo substituent. Instead, in the two metallabicyclic Ir−carbene structures (**Br_C3′$_{PMP}$** and **Br_C4′$_{PMP}$**) located in our calculations, the carbene ligands have a PMP substituent. The only plausible and reasonable explanation for these results is

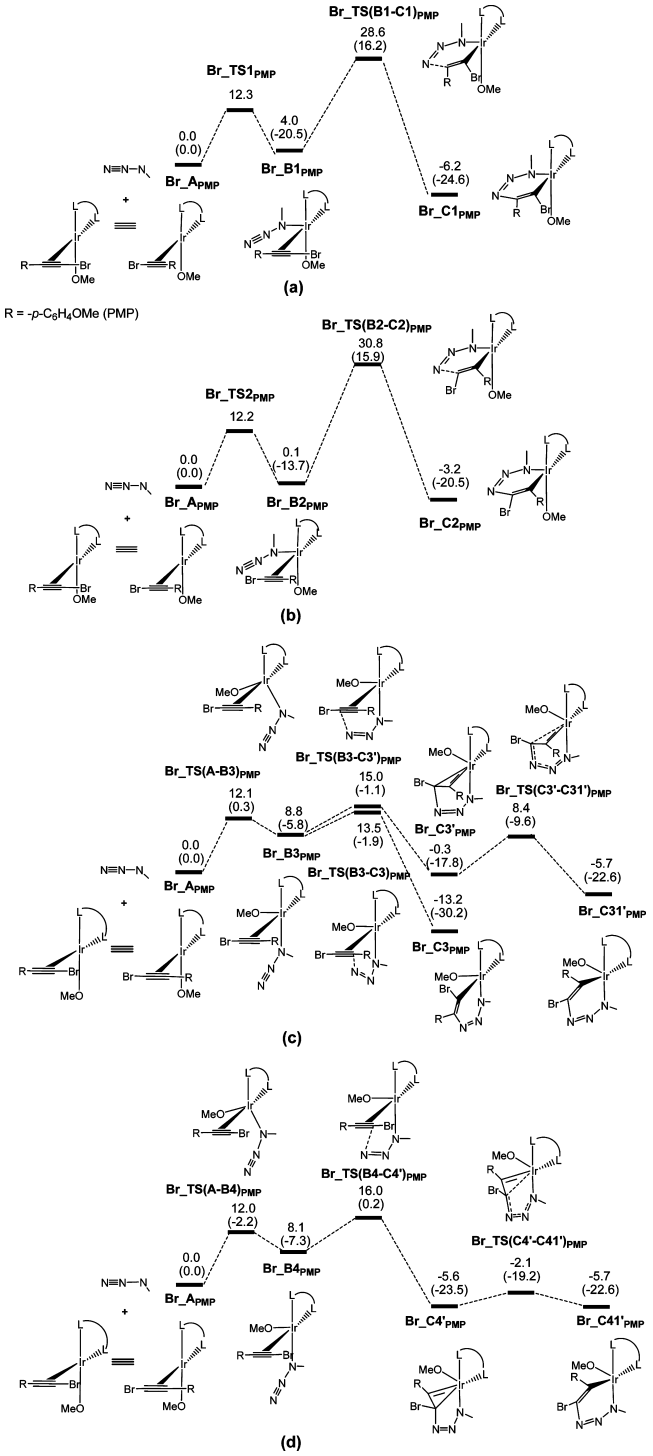

Figure 6. Energy profiles calculated for the oxidative coupling via **Br_B1$_{PMP}$** (a), **Br_B2$_{PMP}$** (b), **Br_B3$_{PMP}$** (c), and **Br_B4$_{PMP}$** (d). Here, the R group is p-C_6H_4OMe, PMP, group. The relative free energies and electronic energies (in parentheses) are given in kcal/mol. **Br_C31′$_{PMP}$** and **Br_C41′$_{PMP}$** are the same species. They are labeled differently for the convenience of discussion.

that a bromo substituent is not an effective substutuent to stabilize such metallabicyclic Ir−carbene structures. Although the π-donating PMP substituent is able to make the two metallabicyclic Ir−carbene structures (**Br_C3′$_{PMP}$** and **Br_C4′$_{PMP}$**) as local minima on the potential energy surface, a PMP substituent is not expected to be a very good

dx.doi.org/10.1021/jo5018348 | J. Org. Chem. 2014, 79, 11970−11980

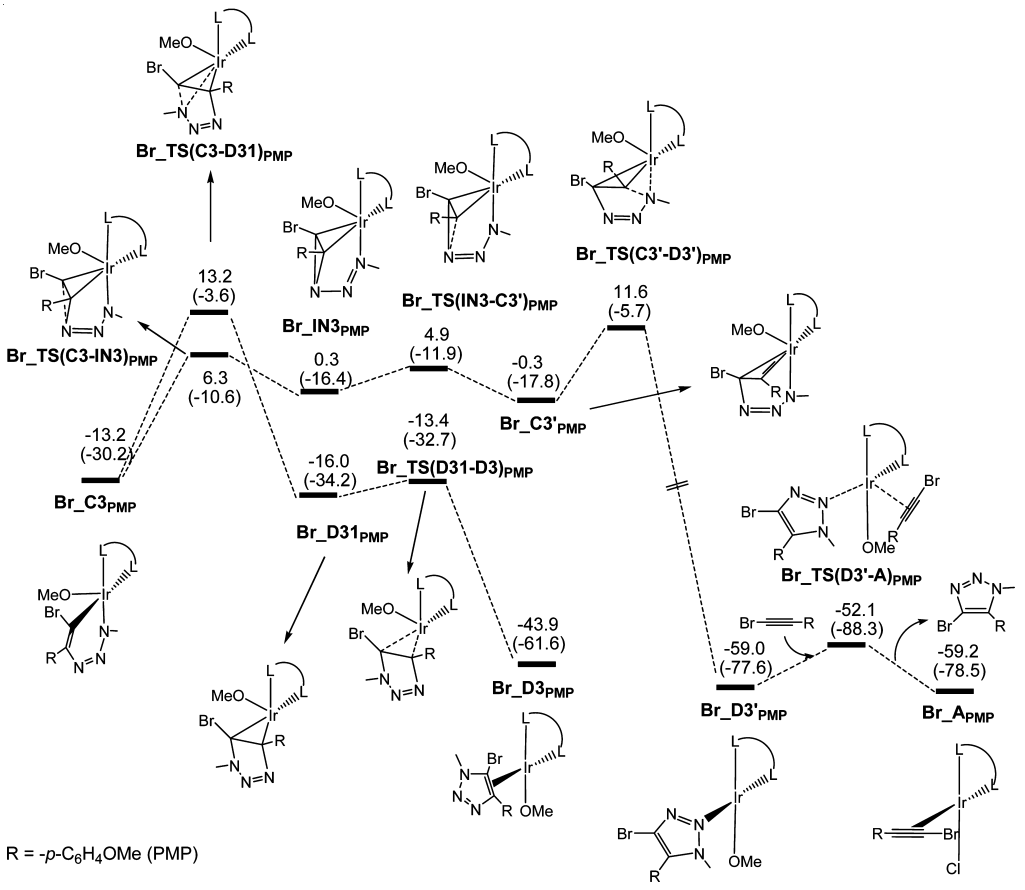

Figure 7. Energy profiles calculated for the cycloaddtion pathway from **Br_C3**$_{PMP}$. The relative free energies and electronic energies (in parentheses) are given in kcal/mol.

substutuent for stabilizing a carbene ligand when compared with an alkylthio/arylthio substituent, as evidenced by the fact that the two metallabicyclic Ir−carbene structures (**Br_C3′**$_{PMP}$ and **Br_C4′**$_{PMP}$) are less stable than the six-membered ring structure **Br_C3**$_{PMP}$. Furthermore, the two metallabicyclic Ir−carbene structures **Br_C3′**$_{PMP}$ and **Br_C4′**$_{PMP}$ can further isomerize to the more stable six-membered ring structures **Br_C31′**$_{PMP}$ and **Br_C41′**$_{PMP}$, respectively (Figure 6c, d). Here, **Br_C31′**$_{PMP}$ and **Br_C41′**$_{PMP}$ are the same species. They are labeled differently for the convenience of discussion.

It is worth commenting on why **Br_C3**$_{PMP}$ is much more stable (by 7.5 kcal/mol) than **Br_C31′**$_{PMP}$ despite the fact that both contain a six-membered ring structure and they only differ in the relative positions of the Br and PMP substituents. The significant energy difference between **Br_C3**$_{PMP}$ and **Br_C31′**$_{PMP}$ is of the following electronic origin. In the structure of **Br_C3**$_{PMP}$ where bromine is bonded to the metal-bonded carbon, the high electronegativity of Br makes the bond between Ir and carbon contain more ionic character and give rise to the high stability for **Br_C3**$_{PMP}$. The NBO analysis shows that natural atomic charges on the Ir and C atoms of the Ir−C bond in **Br_C3**$_{PMP}$ are 0.35e and −0.22e, respectively, while the charges on the corresponding atoms in **Br_C31′**$_{PMP}$ are 0.35e and −0.19e, respectively. These results support the hypothesis that the Ir−C bond in **Br_C3**$_{PMP}$ is more ionic than that in **Br_C31′**$_{PMP}$. To further examine this hypothesis, we calculated the relative energy of the corresponding saturated structures [Ir]−CHBr−CH_2(PMP) and [Ir]−CH(PMP)−CH_2Br ([Ir] = Ir(cod)(OMe)(N_3Me)). The results show that [Ir]−CHBr−CH_2(PMP) is more stable than [Ir]−CH_2−CHBr(PMP) by 7.2 kcal/mol, which confirms our hypothesis. The relative stability of **C41** and **C41′** as well as **C1** and **C2** shown in Figure 2 is also consistent with this hypothesis.

Reductive Elimination. Figure 7 shows the energy profiles calculated for reductive elimination from **Br_C3**$_{PMP}$ to give cycloaddition product. The energy profiles calculated for other less favorable pathways for the Ir-catalyzed cycloaddition reaction of PMPC≡CBr with N_3Me are presented in the Supporting Information. Figure 7 shows that the reductive elimination from **Br_C3**$_{PMP}$ via **Br_TS(C3-D31)**$_{PMP}$ to give 5-bromotriazole regioisomer is less energetically favorable, a result consistent with the experimental observation that 5-bromotriazole was not the major product. The favorable pathway is that **Br_C3**$_{PMP}$ first isomerizes to **Br_C3′**$_{PMP}$ containing a metallabicyclic structure from which reductive elimination gives 4-bromotriazole (experimentally observed).

The results shown in Figure 7 show that favorable reductive elimination is achieved from a metallabicyclic Ir−carbene structure instead from a six-membered ring intermediate. This explains why even though **Br_C3**$_{PMP}$ is the most stable six-membered ring intermediate a direct reductive elimination from it is unfavorable with a free energy barrier of 26.4 kcal/mol (Figure 7). It rather isomerizes to a less stable isomer (**Br_C3′**$_{PMP}$) having a metallabicyclic Ir−carbene structure, from which reductive elimination occurs, giving the experimentally observed product 4-bromotriazole. Further evidence to support the claim here is that direct reductive elimination from the metallabicyclic Ir−carbene structures **Br_C4′**$_{PMP}$

dx.doi.org/10.1021/jo5018348 | J. Org. Chem. 2014, 79, 11970−11980

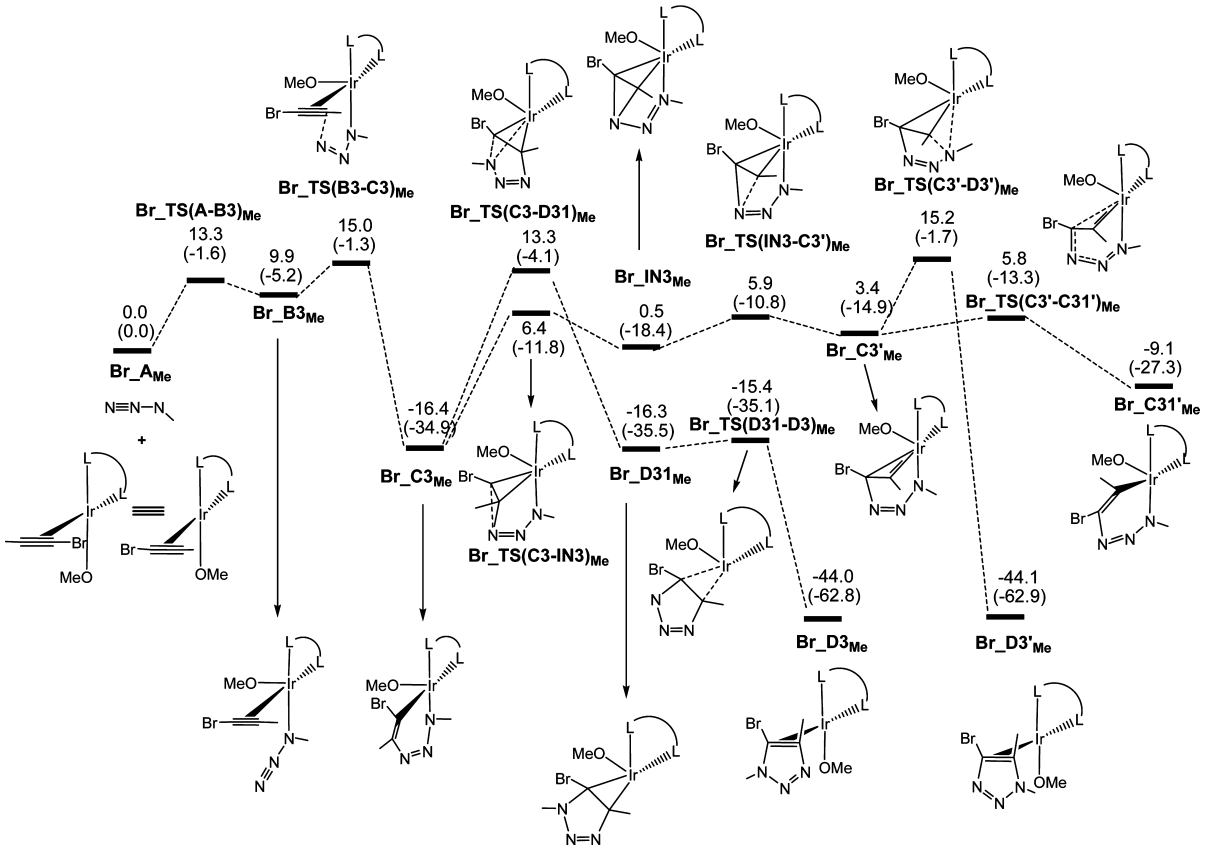

Figure 8. Energy profiles calculated for the iridium-catalyzed cycloaddition of N_3Me with MeC≡CBr via $\mathbf{Br\_B3_{Me}}$. The relative free energies and electronic energies (in parentheses) are given in kcal/mol.

(Figure 6d) to give 4-bromotriazole is also very favorable (with a free energy barrier of only 13.2 kcal/mol from $\mathbf{Br\_C4'_{PMP}}$ to $\mathbf{Br\_TS(C4'\text{-}D41')_{PMP}}$, see the Supporting Information) although the oxidative coupling pathway leading to $\mathbf{Br\_C4'_{PMP}}$ is not the most favorable.

The results discussed above clearly indicate that the experimentally observed regioselectivity is a result of reductive elimination either in $\mathbf{Br\_C3'_{PMP}}$ or $\mathbf{Br\_C4'_{PMP}}$, both of which have a metallabicyclic Ir−carbene structure. The ability of a PMP substituent to effectively stabilize a metallabicyclic Ir−carbene structure is the key for the preferred regioselectivity observed (formation of 4-bromotriazole).

Cycloaddition of MeC≡CBr with N_3Me. Based on the results obtained and discussed above, we hypothesize that a bromoalkyne containing a poorer π-donating substituent (instead of p-C_6H_4OMe) such as MeC≡CBr may give different regioselectivity. Similar to what we have seen in the reaction of PMPC≡CBr, four structural isomers ($\mathbf{Br\_B1_{Me}}$, $\mathbf{Br\_B2_{Me}}$, $\mathbf{Br\_B3_{Me}}$, and $\mathbf{Br\_B4_{Me}}$) were found for the 18-electron species $\mathbf{Br\_B_{Me}}$. From the four isomers, oxidative couplings can take place to give $\mathbf{Br\_C1_{Me}}$, $\mathbf{Br\_C2_{Me}}$, $\mathbf{Br\_C3_{Me}}$, $\mathbf{Br\_C4_{Me}}$, and $\mathbf{Br\_C4'_{Me}}$. The most favorable oxidative coupling pathway again corresponds to that giving the most stable six-membered-ring metallacycle intermediate $\mathbf{Br\_C3_{Me}}$ where the terminal nitrogen of the azide is bonded to the β (methyl-substituted) alkyne carbon.

Figure 8 shows the energy profiles calculated for the favorable pathways for the cycloaddition reaction of MeC≡CBr with N_3Me. The energy profiles for other possible pathways are again presented in the Supporting Information. The result indeed supports the hypothesis that the reaction would favorably give 5-bromotriazole (Figure 8), although experimentally it was found that the reaction of $Me_2C(OH)$-C≡CBr with $(p\text{-}C_6H_4NO_2)CH_2CH_2N_3$ gives 4-bromotriazole.[10] We believe that more experimental work is needed here to further confirm the experimental and theoretical results.

The results shown in Figure 8 are diffirent from what we have seen in Figure 7. Here, the direct reductive elimination in six-membered ring intermediate $\mathbf{Br\_C3_{Me}}$ to give 5-bromotriazole is more favorable than the reductive elimination from the metallabicyclic Ir−carbene intermediate $\mathbf{Br\_C3'_{Me}}$ to give 4-bromotriazole. In $\mathbf{Br\_C3'_{Me}}$, the carbene ligand is stabilized by methyl group via hyperconjugation effect. The stabilization by the hyperconjugation effect is relatively small when compared with that in $\mathbf{Br\_C3'_{PMP}}$, indicating that the transition state $(\mathbf{Br\_TS(C3'\text{-}D3')_{Me}})$ calculated for the reductive elimination from the hyperconjugation-stabilized metallabicyclic Ir−carbene intermediate $\mathbf{Br\_C3'_{Me}}$ is still lying higher in energy than the transition state $(\mathbf{Br\_TS(C3\text{-}D31)_{Me}})$ calculated for the direct elimination in the most stable six-membered ring intermediate $\mathbf{Br\_C3_{Me}}$ (Figure 8).

■ SUMMARY

The detailed mechanisms for the Ir-catalyzed cycloaddition reactions of thioalkynes and bromoalkynes with azides have been investigated with the aid of DFT calculations. The different regioselectivities observed for the two classes of substrates have been discussed and explained. Our calculations have revealed that the cycloaddition reactions of both classes of substrates follow similar yet different reaction mechanisms.

dx.doi.org/10.1021/jo5018348 | J. Org. Chem. 2014, 79, 11970−11980

In the reactions of thioalkynes, the mechanism consists of the following steps (Scheme 2): (i) complexation of alkyne and azide to a three-coordinate Ir(cod)X (X = Cl or OMe) gives a pseudo-square-pyramidal 18-electron Ir species in which X occupies the apical position; (ii) subsequent oxidative coupling between the coordinated thioalkyne and azide through an attack of the terminal azide nitrogen on the alkyne β carbon occurs to give a metallabicyclic Ir−carbene intermediate whose carbene ligand is stabilized by the π-donating alkylthio/arylthio substituent; (iii) reductive elimination in the carbene intermediate leads to the formation of 5-sulfenyltriazole as a ligand; (iv) release of the product and complexation of alkyne and azide regenerate the 18-electron Ir species. The strong π-donating property of the alkylthio/arylthio substituent to effectively stabilize a metallabicyclic Ir−carbene intermediate is the key for the experimentally observed regioselectivity (eq 1).[9]

Scheme 2

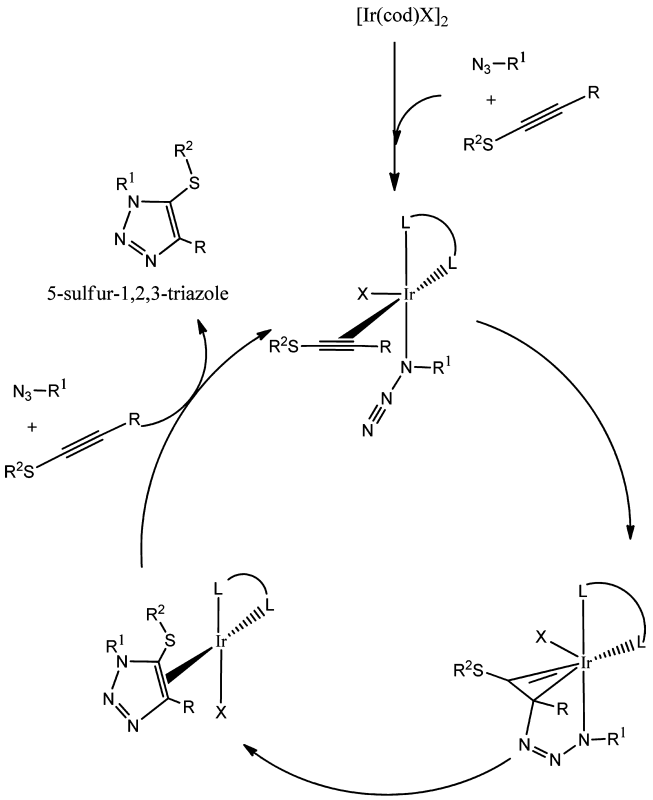

In the reactions of bromoalkynes, the first and last steps are the same as those in the reactions of thioalkynes (Scheme 3). However, the oxidative coupling between the coordinated bromoalkyne and azide through an attack of the terminal azide nitrogen on the alkyne β carbon occurs to give a six-membered-ring intermediate, which does not contain a metallabicyclic Ir−carbene structure as we observed in the reactions of thioalkynes. When R in RC≡CBr is an effective substituent to stabilize a metallabicyclic Ir−carbene species such as the strong π-donating group p-C_6H_4OMe, the six-membered-ring intermediate undergoes isomerization via migrating the terminal azide nitrogen from β carbon to the α carbon to form a metallabicyclic Ir−carbene species whose carbene ligand is stabilized by the p-C_6H_4OMe substituent, from which reductive elimination gives 4-bromotriazole (experimentally observed) as a ligand. When R in RC≡CBr is not a strong π-donating group such as Me, direct reductive elimination in the six-membered-ring intermediate would occur to give 5-bromotriazole (theoretically predicted) as a ligand. The different mechanisms are related to the fact that a bromo substituent is a significantly weaker π-donating substituent than a thio substituent. The preferred regioselectivity for the reactions of bromoalkynes with azides (eq 2) is related to the property of the R substituent.

Scheme 3

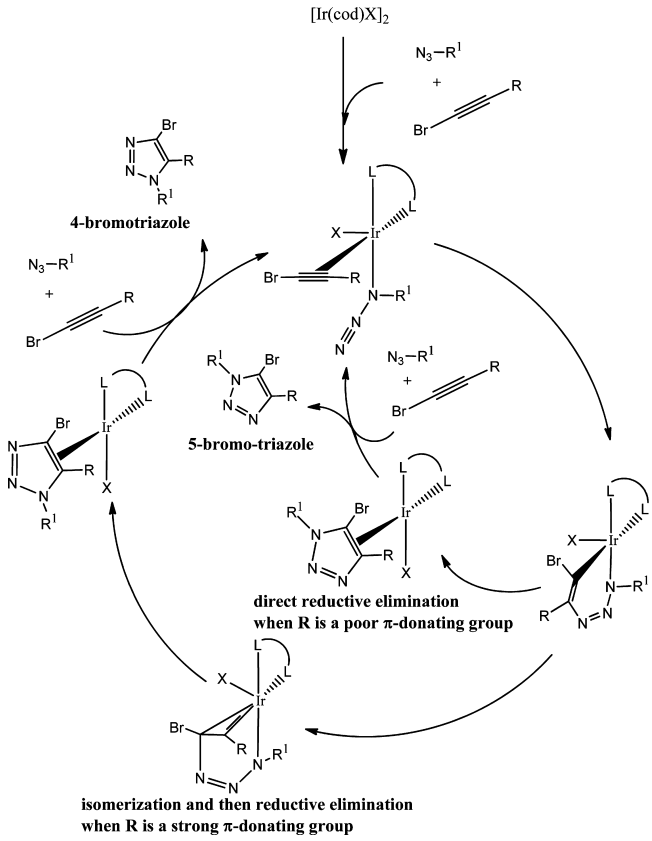

■ ASSOCIATED CONTENT

Ⓢ Supporting Information

Text giving the complete ref 16, relevant energy profiles calculated for the iridium-catalyzed cycloaddition reactions shown in eqs 1 and 2, and tables giving Cartesian coordinates and electronic energies for all of the calculated structures. This material is available free of charge via the Internet at http://pubs.acs.org.

■ AUTHOR INFORMATION

Corresponding Authors

*E-mail: chjiag@ust.hk.
*E-mail: sunjw@ust.hk.
*E-mail: chzlin@ust.hk.

Notes

The authors declare no competing financial interest.

■ ACKNOWLEDGMENTS

This work was supported by the Research Grants Council of Hong Kong (HKUST603313 and CUHK7/CRF/12G) and the Hong Kong Scholars Program (Grant No. XJ2012017).

REFERENCES

(1) (a) For general reviews on chemistry and applications of 1,2,3-triazoles: Fan, W.-Q.; Katritzky, A. R. In *Comprehensive Heterocyclic Chemistry II*; Katritzky, A. R., Rees, C. W., Scriven, E. F. V., Eds.; Elsevier Science: Oxford, U.K., 1996; Vol.4, pp 1−126. (b) Manetsch, R.; Krasiski, A.; Radi, Z.; Raushel, J.; Taylor, P.; Sharpless, K. B.; Kolb, H. C. *J. Am. Chem. Soc.* **2004**, *126*, 12809. (c) Thirumurugan, P.; Matosiuk, D.; Jozwiak, K. *Chem. Rev.* **2013**, *113*, 4905. (d) Wang, J.; Sui, G.; Mocharla, V. P.; Lin, R. J.; Phelps, M. E.; Kolb, H. C.; Tseng, H.-R. *Angew. Chem., Int. Ed.* **2006**, *45*, 5276. (e) Tron, G. C.; Pirali, T.; Billington, R. A.; Canonico, P. L.; Sorba, G.; Genazzani, A. A. *Med. Res. Rev.* **2008**, *28*, 278.

(2) (a) Nandivada, H.; Jiang, X. W.; Lahann, J. *Adv. Mater.* **2007**, *19*, 2197. (b) Lewis, J. E. M.; McAdam, C. J.; Gardinerb, M. G.; Crowley, J. D. *Chem. Commun.* **2013**, *49*, 3398. (c) Golas, P. L.; Matyjaszewski, K. *Chem. Soc. Rev.* **2010**, *39*, 1338.

(3) (a) Rostovtsev, V. V.; Green, L. G.; Fokin, V. V.; Sharpless, K. B. *Angew. Chem., Int. Ed.* **2002**, *41*, 2596. (b) Tornøe, C. W.; Christensen, C.; Meldal, M. *J. Org. Chem.* **2002**, *67*, 3057. (c) Miaoa, T.; Wang, L. *Synthesis* **2008**, 363. (d) Lipshutz, B. H.; Taft, B. R. *Angew. Chem., Int. Ed.* **2006**, *45*, 8235. (e) Shin, J.-A.; Lim, Y.-G.; Lee, K.-H. *J. Org. Chem.* **2012**, *77*, 4117.

(4) (a) Zhang, L.; Chen, X.; Xue, P.; Sun, H. H. Y.; Williams, I. D.; Sharpless, K. B.; Fokin, V. V.; Jia, G. *J. Am. Chem. Soc.* **2005**, *127*, 15998. (b) Rasmussen, L. K.; Boren, B. C.; Fokin, V. V. *Org. Lett.* **2007**, *9*, 5337. (c) Boren, B. C.; Narayan, S.; Rasmussen, L. K.; Zhang, L.; Zhao, H.; Lin, Z.; Jia, G.; Fokin, V. V. *J. Am. Chem. Soc.* **2008**, *130*, 8923. (d) Wang, D.; Salmon, L.; Ruiz, J.; Astruc, D. *Chem. Commun.* **2013**, *49*, 6956.

(5) (a) McNulty, J.; Keskar, K.; Vemula, R. *Chem.—Eur. J.* **2011**, *17*, 14727. (b) Hong, L.; Lin, W.; Zhang, F.; Liu, R.; Zhou, X. *Chem. Commun.* **2013**, *49*, 5589. (c) Wang, Y.-C; Xie, Y.-Y.; Qu, H.-E.; Wang, H.-S.; Pan, Y.-M.; Huang, F.-P. *J. Org. Chem.* **2014**, *79*, 4463.

(6) Worrell, B. T.; Malik, J. A.; Fokin, V. V. *Science* **2013**, *340*, 457.

(7) Himo, F.; Lovell, T.; Hilgraf, R.; Rostovtsev, V. V.; Noodleman, L.; Sharpless, K. B.; Fokin, V. V. *J. Am. Chem. Soc.* **2005**, *127*, 210.

(8) (a) Hein, J. E.; Tripp, J. C.; Krasnova, L. B.; Sharpless, K. B.; Fokin, V. V. *Angew. Chem., Int. Ed.* **2009**, *48*, 8018. (b) Brotherton, W. S.; Clark, R. J.; Zhu, L. *J. Org. Chem.* **2012**, *77*, 6443.

(9) Ding, S.; Jia, G.; Sun, J. *Angew. Chem., Int. Ed.* **2014**, *53*, 1877.

(10) Rasolofonjatovo, E.; Theeramunkong, S.; Bouriaud, A.; Kolodych, S.; Chaumontet, M.; Taran, F. *Org. Lett.* **2013**, *15*, 4698.

(11) Zhao, Y.; Truhlar, D. G. *Theor. Chem. Acc.* **2008**, *120*, 215.

(12) (a) Wadt, W. R.; Hay, P. J. *J. Chem. Phys.* **1985**, *82*, 284. (b) Hays, P. J.; Wadt, W. R. *J. Chem. Phys.* **1985**, *82*, 299.

(13) (a) Fukui, K. J. *Phys. Chem.* **1970**, *74*, 4161. (b) Fukui, K. *Acc. Chem. Res.* **1981**, *14*, 363.

(14) Reed, A. E.; Weinhold, F. *J. Chem. Phys.* **1985**, *83*, 1736.

(15) Marenich, A. V.; Cramer, C. J.; Truhlar, D. G. *J. Phys. Chem. B* **2009**, *113*, 6378.

(16) Frisch, M. J. et al. *Gaussian 09, revision D.01*; Gaussian, Inc., Wallingford CT, 2009.

(17) Albright, T. A.; Burdett, J. K.; Whangbo, M.-H. *Orbital Interactions in Chemistry*, 2nd ed.; John Wiley & Sons: New York, 2013.

(18) Lam, K. C.; Lam, W. H.; Lin, Z.; Marder, T. B.; Norman, N. C. *Inorg. Chem.* **2004**, *43*, 2541.

(19) Cenini, S.; Gallo, E.; Caselli, A.; Ragaini, F.; Fantauzzi, S.; Piangiolino, C. *Coord. Chem. Rev.* **2006**, *250*, 1234.

(20) Hartwig, J. F.; Cook, K. S.; Hapke, M.; Incarvito, C. D.; Fan, Y. B.; Webster, C. E.; Hall, M. B. *J. Am. Chem. Soc.* **2005**, *127*, 2538.

(21) Wei, C. S.; Jiménez-Hoyos, C. A.; Videa, M. F.; Hartwig, J. F.; Hall, M. B. *J. Am. Chem. Soc.* **2010**, *132*, 3078.